made of C, B, and N (with C–N and C–B bonds), rather than a mechanical mixture of graphite and BN. Furthermore, among the three elements present, B in the lattice, with three unpaired electrons that form in-plane σ bonds, has the highest density of unoccupied π orbitals. Correspondingly, the π peak observed in the spectra is the strongest for B, weaker for C (four electrons), and weakest for N (five electrons).

We estimated the B and N concentrations present in the hybrid structures from measurements of the characteristic signals after background subtraction. The involved cross sections were calculated with the usual σ-K hydrogenic model (*15*). We always found that B and N were present in the samples in a 1:1 ratio (for all concentrations), which confirms the substitution of the elements into the C network in the (B_xN_x) stoichiometry. However, in some samples taken from the soot that forms in the outer and colder regions of the chamber, EELS structures corresponding to amorphous B were seen with little trace of N. In some cases we observed the stoichiometry C_2BN, matching the composition obtained for CVD-made CBN, but in the majority of cases the average composition corresponded to $C_yB_xN_x$, where $y \gg x$. However, because the electron beam probes local areas, the possibility exists that local areas (nanometers) with C_2BN stoichiometry are surrounded by pure graphite.

Energy-loss line spectra (*3*, *16*) taken from different structures confirm that BN is not deposited as an impurity on the surfaces. Line scans from tubes show that the profiles of the B and N peaks follow shapes similar to that in multilayer tubes, although the shapes are not smooth as we had reported for pure C tubes (*3*). This could be because the presence of B and N is not uniform along the length or cross section of the tubes and the substitution is spatially random. However, in tubes the doping is higher in the outer layers (Fig. 4 inset). Concentration profiles of B and N in some tubes resemble an outer carbonated BN coating (few layers) for the inner BN-substituted (small amounts) C tubes. The concentrations of B and N are highest in some of the sheets. The line scans across thin planar CBN sheets clearly show (Fig. 4) that the amounts of B (also N) and C present are spatially very well anticorrelated, confirming doping by substitution. The limiting spatial extent of this anticorrelation is of the order of 2 to 3 nm, and the existence of local domains of pure phases with dimensions of this order is quite probable. However, the anticorrelation in the intensity of the EELS peaks proves clearly that the missing C atoms in graphitic networks are replaced and shared by B and N. The same is observed for the tubes.

Our observations of the growth of B- and N-substituted graphitic and nanotube structures during the electric arc-discharge process is surprising because it has been shown that CBN phases and a mixture of BN and graphite are unstable when annealed (slowly) to temperatures higher than 2000°C and that they decompose to boron carbide and graphite, releasing nitrogen (*12*). The temperatures that exist in the region where the deposits are formed during the arc-discharge process is >3500°C. In fact, in the outer regions of the chamber where the temperatures are lower, no doping is observed. One possible explanation for the formation of B- and N-substituted graphite, as discussed by others (*12*), could be the extremely small time scales involved in the reactions in the C plasma; the formation reaction of CBN could occur at a much faster rate than the decomposition reaction to form the carbide phase and nitrogen. Also, because the reaction is carried out in a nitrogen ambient, the equilibrium reaction rates might be shifted in a way that favors CBN formation at elevated temperatures.

REFERENCES AND NOTES

1. W. Kratschmer, L. D. Lamb, K. Fostiropoulos, D. R. Huffman, *Nature* **347**, 354 (1990).
2. S. Iijima, *ibid.* **354**, 54 (1991); T. W. Ebbesen and P. M. Ajayan, *ibid.* **358**, 220 (1992).
3. P. M. Ajayan *et al.*, *Phys. Rev. Lett.* **72**, 1722 (1993).
4. R. S. Rouff, D. C. Lorents, B. Chan, R. Malhotra, S. Subramoney, *Science* **259**, 346 (1993); M. Tomita, Y. Saito, T. Hayashi, *Jpn. J. Appl. Phys.* **32**, L280 (1993).
5. M. S. Dresselhaus, G. Dresselhaus, K. Sugihara, I. L. Spain, H. A. Goldberg, in *Graphite Fibers and Filaments*, M. Cardona, Ed. (Springer, Berlin, 1988), pp. 244–286.
6. A. R. Badzian, S. Appenheimer, T. Niemyski, E. Olkusnik, in *Proceedings of the Third International Conference on Chemical Vapor Deposition*, F. A. Glaski, Ed. (American Nuclear Society, Hindsdale, IL, 1972), p. 747–752; R. B. Kaner, J. Kouvetakis, C. E. Warble, M. L. Sattler, N. Bartlett, *Mater. Res. Bull.* **22**, 399 (1987).
7. E. J. M. Hamilton *et al.*, *Science* **260**, 659 (1993).
8. J.-Y. Yi and J. Bernholc, *Phys. Rev. B* **47**, 1708 (1993); A. Rubio, J. L. Corkill, M. L. Cohen, *ibid.* **49**, 5081 (1994); Y. Miyamoto, A. Rubio, M. L. Cohen, S. G. Louie, *ibid.* **50**, 4976 (1994).
9. T. Guo, C. Jin, R. E. Smalley, *J. Phys. Chem.* **95**, 4948 (1991).
10. A. Y. Liu, R. M. Wentzcovitch, M. L. Cohen, *Phys. Rev. B* **39**, 1760 (1989).
11. Thicker tubes often show three-dimensional graphitic regions in the cores and edges, as seen from the splitting of (100) and (101) reflections in diffraction patterns and the presence of (*hkℓ*) spots. Diffraction from most thin long filaments only shows (001) spots [large values of ℓ, up to 12, are sometimes seen suggesting preferential orientation of the (002) planes along the cross section of tubes or flattened tubes] and (*hk*0) rings suggesting tubular morphology (*2*). Diffraction also shows the superposition of deformed ellipses for (*hk*0) rings, which have been shown to arise from tubes with polygonal facets [M. Liu and J. M. Cowley, *Ultramicroscopy* **53**, 333 (1994)]. The (*hk*0) rings from the tubes extend in the reciprocal space radially, suggesting possible variations in the in-plane spacing, which could depend on the composition of the network (*12*); but elongation of spots is also indicative of the fibrous structure.
12. A. W. Moore *et al.*, *J. Appl. Phys.* **65**, 5109 (1989); F. Saugnac, F. Teyssandier, A. Marchand, *J. Am. Ceram. Soc.* **75**, 161 (1992).
13. J. Kouvetakis, *et al.*, *Synth. Metals* **34**, 1 (1989).
14. H. Kurata, E. Lefevre, C. Colliex, R. Brydson, *Phys. Rev. B* **47**, 13763 (1993).
15. R. F. Egerton, *EELS in the Electron Microscope* (Plenum, New York, 1986).
16. C. Colliex, *et al.*, *Mikrochim. Acta* **114–115**, 71 (1994).

16 August 1994; accepted 5 October 1994

The Stereochemical Course of Group II Intron Self-Splicing

Richard A. Padgett,* Mircea Podar, Scott C. Boulanger, Philip S. Perlman

The stereochemical specificities and reaction courses for both self-splicing steps of a group II intron have been determined by phosphorothioate substitution at the 5′ and 3′ splice site phosphodiester bonds. Both steps of the splicing reaction proceeded with a phosphorothioate in the *Sp* configuration but were blocked by the *Rp* diastereomer. Both steps also proceeded with inversion of stereochemical configuration around phosphorus, consistent with a concerted transesterification reaction. These results are identical to those found for nuclear precursor mRNA (pre-mRNA) splicing and provide support for the hypothesis that group II introns and nuclear pre-mRNA introns share a common evolutionary history.

Recent work has defined the stereochemical course of nuclear pre-mRNA splicing by means of site-specific substitutions of nonbridging oxygens with sulfur at the splice-junction phosphodiester bonds (*1*, *2*). This substitution produces a chiral center at the phosphorus with two configurations denoted *Sp* and *Rp*. The normal oxygen atoms at the prochiral-*Rp* and prochiral-*Sp* positions frequently interact differently with enzymes and ribozymes (*3*). Thus, the analysis of the effects of substitution at these positions can define features of the catalytic site, and anal-

Department of Biochemistry, University of Texas Southwestern Medical Center at Dallas, 5323 Harry Hines Boulevard, Dallas, TX 75235, USA.

*To whom correspondence should be addressed.

ysis of the stereochemical configuration of the product of a phosphotransfer reaction involving a chiral substrate can help define the chemical course of the reaction. From such analyses, pre-mRNA splicing has been shown to proceed with *Sp* phosphorothioates at either splice site but to be blocked by *Rp* phosphorothioates, and that both splicing steps proceed through inversion of stereochemical configuration (*1*, *2*). These results have been interpreted as meaning that the prochiral-*Rp* oxygen of the phosphodiester bond that is cleaved in the reaction interacts with an element of the active site, possibly a magnesium ion, that is critical for activity (*4*). That both steps have the same stereospecificity suggests that the second is not the reverse of the first. Thus, each step may be catalyzed by a distinct active site (*2*). In contrast, group I introns use an *Rp* phosphorothioate at the 5′ splice site, and an *Sp* phosphorothioate at the 3′ splice site, which reinforces the view that the second step of group I splicing is mechanistically a reversal of the first and that a single active site is involved (*5*).

Group II self-splicing introns use a two-step transesterification reaction mechanism with formation of a branched lariat RNA, which is identical to the mechanism used by nuclear pre-mRNA spliceosomal introns (*6*). Thus, it was of interest to determine if the similarities of group II and nuclear pre-mRNA splicing mechanisms extend to the level of the organization of their catalytic active sites. To obtain group II intron precursor RNAs with single, stereochemically defined phosphorothioate substitutions at the 5′ and 3′ splice junctions, we joined chemically synthesized RNA oligonucleotides containing single, stereochemically defined phosphorothioate substitutions to in vitro RNA transcripts using DNA-mediated ligation to produce complete self-splicing group II introns (Fig. 1).

A complete self-splicing RNA derived from the yeast mitochondrial aI5γ group II intron was created by a three-part ligation involving an enzymatically synthesized exon 1, a chemically synthesized 5′ splice junction oligonucleotide, and an enzymatically synthesized labeled RNA comprising the balance of the intron plus exon 2 (Fig. 1A). Purified, ligated molecules were reacted under self-splicing conditions where the predominant reaction pathway is by branching to the 2′ hydroxyl of a specific adenosine residue in domain VI of the intron (*7*).

The results of this experiment show that branch formation is evident for the control oxygen and the *Sp* phosphorothioate RNAs but is seen at only a very low level in the *Rp* phosphorothioate RNA (Fig. 2). This low level is due to a small contamination of the *Rp* phosphorothioate oligonucleotide with the oxygen-containing species (*8*). Thus, the first step of group II intron self-splicing shows the same stereospecificity as pre-mRNA splicing. Another result apparent from the quantitation of the reactions in Fig. 2 is that the reaction rate of the *Sp* phosphorothioate–substituted RNA in step 1 is significantly slower than that of the unsubstituted RNA (*9*).

To analyze the stereochemical requirements of step 2 of group II intron self-splicing, RNAs with either an oxygen or a sulfur in the *Rp* or *Sp* configuration at the 3′ splice site were constructed (Fig. 1B). As shown in Fig. 3, step 1 of the splicing reaction proceeded with all three substrates, as evidenced by the production of lariat intermediate molecules. The second step of the reaction, which produces the spliced exon RNA, proceeded when the 3′ splice junction contained either an oxygen or an *Sp* phosphorothioate but was blocked by the presence of an *Rp* phosphorothioate. These results show that both steps of group II intron self-splicing proceed with *Sp* phosphorothioates but are blocked by the *Rp* diastereomer, the same specificity as is seen in nuclear pre-mRNA splicing.

All of the splicing reactions tested to date appear to use a similar mechanism that results in the inversion of the stereochemical configuration around phosphorus (*1*, *2*, *5*). This inversion is consistent with an S_N2-type in-line transesterification reaction that proceeds through a trigonal bipyramidal intermediate with the attacking and leaving groups in the apical positions.

To determine if group II intron self-splicing follows this pattern, we analyzed the

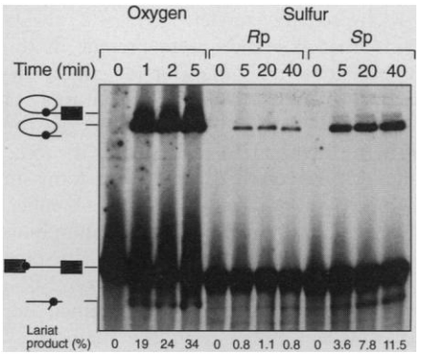

Fig. 2. Analysis of the stereospecificity of step 1 of self-splicing. RNAs containing oxygen or sulfur in the *Rp* or *Sp* configuration at the 5′ splice junction were reacted under self-splicing conditions for the times indicated and separated by denaturing polyacrylamide gel electrophoresis (*18*). The positions of lariat intermediate, lariat product, precursor, and broken lariat RNA species are indicated. The intron was labeled in this precursor RNA so that the spliced exon product is not observed. Analogous experiments with differently labeled substrate RNA showed that spliced exon RNA is produced in equimolar amounts to excised intron RNA (*12*). The extent of reaction for each point is listed at the bottom of the lane as a percentage of the input RNA.

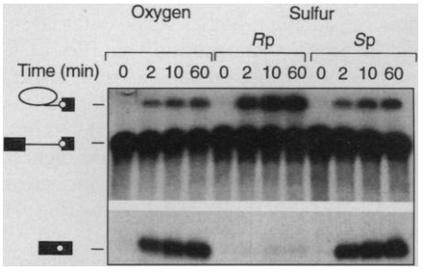

Fig. 3. Analysis of the stereospecificity of step 2 of self-splicing. RNAs containing oxygen or sulfur in the *Rp* or *Sp* configuration at the 3′ splice junction were reacted under self-splicing conditions for the times indicated and separated by denaturing polyacrylamide gel electrophoresis (*18*). The positions of lariat intermediate, precursor, and spliced exon product RNAs are indicated. The second exon was labeled in this reaction so that the lariat intron product and the first exon intermediate are not observed. The regions of the gel shown contained the only bands present.

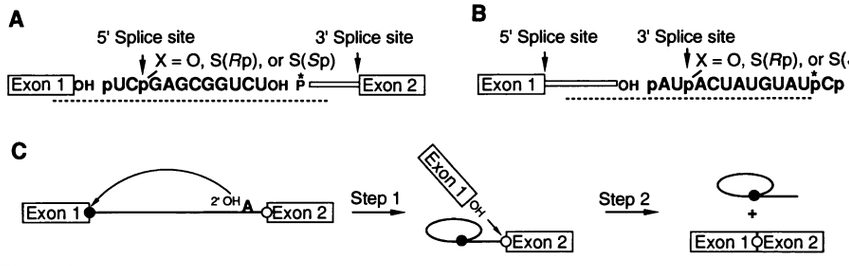

Fig. 1. Scheme for the site-specific insertion of stereochemically defined phosphorothioates into group II intron splicing substrates. Chemically synthesized oligonucleotides (bold type) (*15*) were ligated to enzymatically transcribed RNAs with a bridging DNA oligonucleotide (dotted line) and T4 DNA ligase. The sites and fates of the sulfur atoms are marked by circles. Labeled phosphorus atoms are marked with asterisks. (**A**) Construction of 5′ splice site–modified self-splicing RNAs (*16*). (**B**) Construction of 3′ splice site–modified self-splicing RNAs (*17*). (**C**) These RNAs were then spliced to yield the intermediates and products diagrammed. The sulfur at the 5′ splice site becomes part of the 2′-5′ phosphorothioate bond in the branch structure of the lariat product RNA, and the sulfur at the 3′ splice site becomes part of the phosphorothioate linkage between the two exons in the product RNA.

stereochemical outcomes of the two splicing steps. In step 1 of the reaction, the sulfur atom from the 5′ splice junction is incorporated into the 2′-5′ phosphodiester bond formed between the branch site adenosine and the 5′ end of the intron (Fig. 1C). To determine if the sulfur derived from the active Sp isomer is in the *Rp* or the *Sp* configuration, we isolated branch core trinucleotides from spliced intron RNA from either control oxygen or Sp phosphorothioate–substituted precursor RNAs by nuclease P1 digestion and preparative gel electrophoresis. This trinucleotide was then treated with snake venom phosphodiesterase (SVPD), which preferentially cleaves *Rp* phosphorothioate bonds (*10*). If the configuration of the Sp phosphorothioate at the 5′ splice junction was inverted to *Rp*, only mononucleotides would be released from the branch core by SVPD. If the Sp configuration was retained, a labeled dinucleotide would be seen. As shown in Fig. 4A, only mononucleotides were released by SVPD digestion, showing that the Sp phosphorothioate in the substrate RNA was inverted during the splicing reaction to *Rp*. Control experiments show that a synthetic Sp phosphorothioate dinucleotide was uncleaved under identical conditions (see Fig. 5C, lane 9).

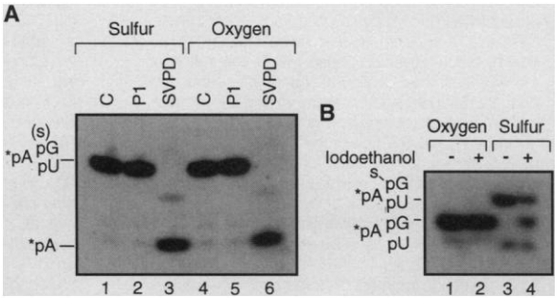

Fig. 4. Analysis of the stereochemical configuration of the products of step 1 of group II intron self-splicing. Complete self-splicing RNAs containing either oxygen or an Sp phosphorothioate at the 5′ splice site were prepared as in Fig. 1A except that the intron–exon 2 RNA used in the ligations was transcribed in the presence of [α-^{32}P]ATP (adenosine triphosphate) to label the adenosine at the branch site in domain VI. These RNAs were spliced and digested with nuclease P1, and the resistant branch trinucleotides were isolated from a preparative 25% acrylamide gel (*1*). The labeled phosphorus is indicated by the asterisk. (**A**) Lanes 1 to 3, phosphorothioate-containing (sulfur) branched trinucleotide; lanes 4 to 6, control (oxygen) branched trinucleotide. Each set of lanes contains trinucleotide either unreacted (C, lanes 1 and 4), digested with nuclease P1 (lanes 2 and 5), or digested with SVPD (lanes 3 and 6) (*19*). Reactions were analyzed on a 25% denaturing polyacrylamide gel. Positions of the various substrates and products are shown. (**B**) Effect of iodoethanol on control and phosphorothioate-containing branch trinucleotides. Lane 1, untreated control trinucleotide; lane 2, control trinucleotide treated with iodoethanol; lane 3, untreated phosphorothioate-containing trinucleotide; and lane 4, phosphorothioate-containing trinucleotide treated with iodoethanol. Samples were analyzed on a 25% polyacrylamide gel without urea.

Figure 4B shows that the branch core used in Fig. 4A contains a sulfur atom, because it migrated more slowly on a nondenaturing gel than did the control oxygen species (*1, 2*), and this mobility difference was lost when the sulfur was removed by treatment with iodoethanol (*11*). Further evidence that the sulfur atom was present in the 2′-5′ bond is that the lariat product RNA from the Sp phosphorothioate RNA was resistant to cleavage by the HeLa cell debranching activity (*1*), whereas the control oxygen lariat was cleaved (*12*). Thus, step 1 of group II intron self-splicing occurs through inversion around phosphorus.

In step 2 of splicing, the sulfur from the 3′ splice site is incorporated into the phosphodiester bond linking the two ligated exons (Fig. 1C). To determine the stereochemical configuration of this bond, we constructed complete cis-splicing RNAs in which the only labeled phosphorus was located one nucleotide 5′ of the 5′ splice site and which contained either a phosphodiester or an Sp phosphorothioate bond at the 3′ splice site. In the spliced exon product, this label will be located one nucleotide 5′ of the phosphodiester or phosphorothioate bond formed during ligation of the exons. Thus, cleavage of the spliced exon product by stereospecific nucleases that leave 5′ phosphate termini will produce either labeled dinucleotide or mononucleotide products depending on the stereochemistry of the bond produced by step 2 of splicing (Fig. 5A). Digestion of the spliced exon product RNA from the Sp phosphorothioate–substituted RNA with nuclease P1 gave a resistant dinucleotide species (Fig. 5B, lane 4), whereas digestion of the control oxygen-containing spliced exon product RNA produced only mononucleotides (Fig. 5B, lane 2). Further digestion of the phosphorothioate-containing dinucleotide with SVPD produced only mononucleotide products (Fig. 5B, lane 5). Nuclease P1

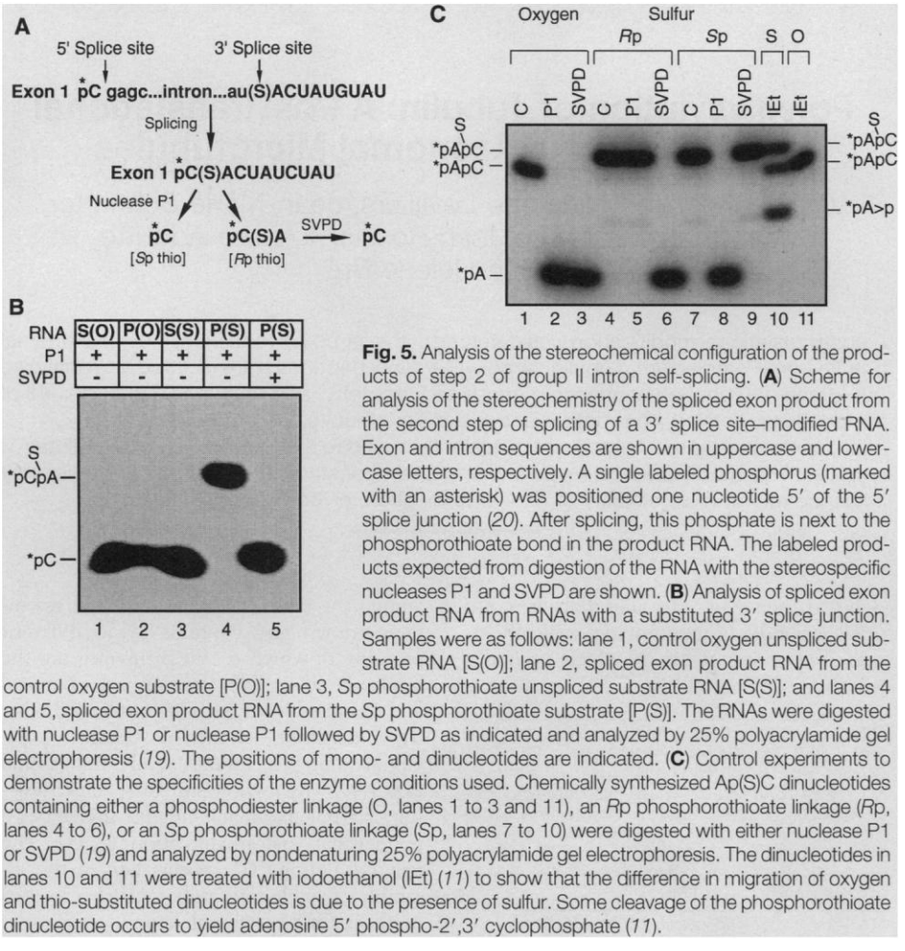

Fig. 5. Analysis of the stereochemical configuration of the products of step 2 of group II intron self-splicing. (**A**) Scheme for analysis of the stereochemistry of the spliced exon product from the second step of splicing of a 3′ splice site–modified RNA. Exon and intron sequences are shown in uppercase and lowercase letters, respectively. A single labeled phosphorus (marked with an asterisk) was positioned one nucleotide 5′ of the 5′ splice junction (*20*). After splicing, this phosphate is next to the phosphorothioate bond in the product RNA. The labeled products expected from digestion of the RNA with the stereospecific nucleases P1 and SVPD are shown. (**B**) Analysis of spliced exon product RNA from RNAs with a substituted 3′ splice junction. Samples were as follows: lane 1, control oxygen unspliced substrate RNA [S(O)]; lane 2, spliced exon product RNA from the control oxygen substrate [P(O)]; lane 3, Sp phosphorothioate unspliced substrate RNA [S(S)]; and lanes 4 and 5, spliced exon product RNA from the Sp phosphorothioate substrate [P(S)]. The RNAs were digested with nuclease P1 or nuclease P1 followed by SVPD as indicated and analyzed by 25% polyacrylamide gel electrophoresis (*19*). The positions of mono- and dinucleotides are indicated. (**C**) Control experiments to demonstrate the specificities of the enzyme conditions used. Chemically synthesized Ap(S)C dinucleotides containing either a phosphodiester linkage (O, lanes 1 to 3 and 11), an *Rp* phosphorothioate linkage (*Rp*, lanes 4 to 6), or an *Sp* phosphorothioate linkage (*Sp*, lanes 7 to 10) were digested with either nuclease P1 or SVPD (*19*) and analyzed by nondenaturing 25% polyacrylamide gel electrophoresis. The dinucleotides in lanes 10 and 11 were treated with iodoethanol (IEt) (*11*) to show that the difference in migration of oxygen and thio-substituted dinucleotides is due to the presence of sulfur. Some cleavage of the phosphorothioate dinucleotide occurs to yield adenosine 5′ phospho-2′,3′ cyclophosphate (*11*).

cleaves *Sp* phosphorothioate bonds but not *Rp* bonds (*13*), whereas SVPD shows the opposite specificity (*10*). Control experiments with chemically synthesized phosphorothioate dinucleotides showed that these enzymes cleaved with the expected stereospecificity under identical conditions (Fig. 5C). These results show that the *Sp* phosphorothioate in the substrate RNA was inverted to *Rp* in the second step of group II self-splicing.

Much has been written about the apparent similarities between the structures and splicing mechanisms of group II and pre-mRNA introns (*14*). These similarities could be due to a common evolutionary origin or due to chemical determinism driven by a need to carry out similar reactions. Our data extend the similarities to the level of the stereochemistry of the fundamental reactions of these introns and provide strong support for a close relation between these two classes of introns. Because group II intron ribozymes carry out the same chemical reactions as in pre-mRNA splicing but without the need to assemble a spliceosome from trans-acting factors, they might represent a more accessible system in which to investigate the details of these reactions.

REFERENCES AND NOTES

1. K. L. Maschhoff and R. A. Padgett, *Nucleic Acids Res.* **21**, 5456 (1993).
2. M. J. Moore and P. A. Sharp, *Nature* **365**, 364 (1993).
3. F. Eckstein, *Annu. Rev. Biochem.* **54**, 367 (1985).
4. T. A. Steitz and J. A. Steitz, *Proc. Natl. Acad. Sci. U.S.A.* **90**, 6498 (1993); M. Yarus, *FASEB J.* **7**, 31 (1993).
5. J. Rajagopal, J. A. Doudna, J. W. Szostak, *Science* **244**, 692 (1989); J. A. McSwiggen and T. R. Cech, *ibid.*, p. 679; E. Suh and R. B. Waring, *Nucleic Acids Res.* **20**, 6303 (1992).
6. P. S. Perlman, C. L. Peebles, C. Daniels, in *Intervening Sequences in Evolution and Development*, E. M. Stone and R. J. Schwartz, Eds. (Oxford Univ. Press, New York, 1990), pp. 112–161; C. Guthrie, *Science* **253**, 157 (1991).
7. K. A. Jarrell, C. L. Peebles, R. C. Dietrich, S. L. Romiti, P. S. Perlman, *J. Biol. Chem.* **263**, 3432 (1988).
8. The *Rp* phosphorothioate oligonucleotide contained 1.5% phosphodiester oligonucleotide as determined by analytical high-pressure liquid chromatography (HPLC). The level of splicing seen with the *Rp* phosphorothioate-substituted RNA is consistent with this level of purity. The final extents of the splicing reactions at 7.5 hours were *Rp*, 2 to 4%; *Sp*, 80 to 85%; and oxygen, 95 to 98%.
9. Preliminary experiments show that the reduction in the initial rate of reaction on *Sp* phosphorothioate substitution is at least 30-fold. Further experiments show that addition of $MnCl_2$ to the *Sp* reaction enhanced the rate of this reaction without affecting the rate of reaction of the unsubstituted RNA. These results suggest that one or more divalent metal ions are involved in contacts with the prochiral-*Sp* oxygen. Similar experiments with the *Rp* phosphorothioate-substituted RNAs at either splice junction showed no detectable reaction on addition of $MnCl_2$.
10. P. M. Burgers and F. Eckstein, *Proc. Natl. Acad. Sci. U.S.A.* **75**, 4798 (1978); P. S. Nelson, C. T. Bach, J. P. H. Verheyden, *J. Org. Chem.* **49**, 2314 (1984); A. D. Griffiths, B. V. L. Potter, I. C. Eperon, *Nucleic Acids Res.* **15**, 4145 (1987).
11. G. Gish and F. Eckstein, *Science* **240**, 1520 (1988).
12. M. Podar, P. S. Perlman, R. A. Padgett, unpublished data.
13. B. V. L. Potter, B. A. Connolly, F. Eckstein, *Biochemistry* **22**, 1369 (1983).
14. P. A. Sharp, *Cell* **42**, 397 (1985); T. R. Cech, *ibid.* **44**, 207 (1986); A. Jacquier, *Trends Biochem. Sci.* **15**, 351 (1991); A. M. Weiner, *Cell* **72**, 161 (1993).
15. Oligonucleotides containing single sites of phosphorothioate modification were synthesized, modified, and purified as described (*1*) except that the initial product was purified by HPLC on a SAX column [G. Slim and M. J. Gait, *Nucleic Acids Res.* **19**, 1183 (1991)] before reversed-phase HPLC separation of the isomers. The configurations of the separated phosphorothioate isomers were verified by comparing the products of digestion with nuclease P1, ribonuclease A, and SVPD, which have established stereospecificities for cleavage of phosphorothioates. The sequence of the 5′ splice junction oligonucleotide was 5′-UC(S)GAGCGGUCU, where (S) denotes the position of sulfur substitution. The sequence of the 3′ splice junction oligonucleotide was 5′-AU-(S)ACUAUGUAU.
16. A 68-nucleotide fragment of exon 1 ending two nucleotides before the 5′ splice junction was transcribed with T7 RNA polymerase from a polymerase chain reaction (PCR)–generated template. This was ligated to the synthetic 11-nucleotide 5′ splice junction RNA by means of DNA-mediated ligation [(*1*) and M. J. Moore and P. A. Sharp, *Science* **256**, 992 (1992)]. The ligated product was purified by preparative gel electrophoresis. To generate the complete intron RNA, we ligated this E1 + oligonucleotide RNA to a 938-nucleotide RNA beginning 10 nucleotides downstream of the 5′ splice junction and continuing through 60 nucleotides of the second exon. This RNA was made by T7 RNA polymerase transcription of a PCR-generated template, dephosphorylated with calf intestinal phosphatase, and labeled at the 5′ end with T4 polynucleotide kinase and [γ-^{32}P]adenosine triphosphate (ATP). The full-length intron RNA was purified by preparative gel electrophoresis.
17. Synthetic 11-nucleotide 3′ splice junction RNAs were 3′ end-labeled with ^{32}P pCp with T4 RNA ligase and then joined by means of DNA-mediated ligation to a T7 RNA polymerase transcript containing the 5′ exon and the entire intron ending two nucleotides before the 3′ splice junction. The ligated product was purified by preparative gel electrophoresis.
18. Splicing reactions were carried out in 0.5 M $(NH_4)_2SO_4$, 100 mM $MgCl_2$, 1 mM dithiothreitol, and 40 mM Hepes buffer (pH 7.3) at 45°C (*7*). Products were analyzed on a 4% polyacrylamide gel containing 8 M urea and quantitated on a Molecular Dynamics PhosphorImager.
19. Samples were digested with 3.3×10^{-3} units of SVPD (Type I, Sigma) in 10 mM tris-HCl (pH 8.0), 1 mM EDTA, and 5 mM Na_2PO_4 with 1 μg of tRNA for 60 min at 37°C or 20 ng of nuclease P1 in 15 mM ammonium acetate (pH 4.6) with 1 μg of tRNA for 60 min at 37°C. Iodoethanol treatment was as described (*11*), which in the absence of a free 2′ hydroxyl group results mainly in desulfurization of the phosphorothioate.
20. RNAs containing either a phosphodiester bond or an *Sp* phosphorothioate bond at the 3′ splice site and containing a single labeled phosphorus one position 5′ of the 5′ splice site were prepared as follows: an exon 1 RNA ending at position −1 was ligated to a 5′ ^{32}P-labeled RNA transcript of the entire intron initiated with CpG, which ended at position −2 from the 3′ splice site. This labeled RNA was then ligated to either the control oxygen, *Rp* phosphorothioate, or *Sp* phosphorothioate 3′ splice site oligonucleotide. These RNAs were spliced and digested with nuclease P1 or SVPD as above.

21. Supported by NIH grants GM31480 (P.S.P.) and GM45371 (R.A.P.) and Welch Foundation grants I-1211 (P.S.P.) and I-1035 (R.A.P.).

3 August 1994; accepted 18 October 1994

Polyglycylation of Tubulin: A Posttranslational Modification in Axonemal Microtubules

Virginie Redeker, Nicolette Levilliers, Jean-Marie Schmitter, Jean-Pierre Le Caer, Jean Rossier,* André Adoutte, Marie-Hélène Bré

A posttranslational modification was detected in the carboxyl-terminal region of axonemal tubulin from *Paramecium*. Tubulin carboxyl-terminal peptides were isolated and analyzed by Edman degradation sequencing, mass spectrometry, and amino acid analysis. All of the peptides, derived from both α and β tubulin subunits, were modified by polyglycylation, containing up to 34 glycyl units covalently bound to the γ carboxyl group of glutamyl residues. This modification, present in one of the most stable microtubular systems, may influence microtubule stability or axoneme function, or both.

The axoneme of cilia and flagella comprises a bundle of microtubules typically arranged as a ring of nine doublets around a pair of single microtubules. This structure is among the most stable microtubular assemblies known and contains >150 different proteins, of which α and β tubulins are the most abundant (*1*). Immunocytochemical and immunoblotting studies with antibodies to *Paramecium* axonemal tubulin—polyclonal anti-PA tubulin and monoclonal AXO 49, which show similar specificities—suggest that axonemal tubulin undergoes a posttranslational modification (*2*, *3*). The reactive epitope (i) appears late in the assembly of stable microtubules, (ii) is located in the COOH-terminal domain of both α

V. Redeker, J.-P. Le Caer, J. Rossier, Institut Alfred Fessard, CNRS Unité Propre de Recherche 2212, 91198 Gif-sur-Yvette Cedex, France.
N. Levilliers, A. Adoutte, M.-H. Bré, Laboratoire de Biologie Cellulaire 4, CNRS Unité de Recherche Associée 1134, Université Paris XI, 91405 Orsay Cedex, France.
J.-M. Schmitter, Laboratoire de Biochimie, CNRS Unité de Recherche Associée 240, Ecole Polytechnique, 91128 Palaiseau Cedex, France.

*To whom correspondence should be addressed.